Available online on 15.11.2025 at http://jddtonline.info

Journal of Drug Delivery and Therapeutics

Open Access to Pharmaceutical and Medical Research

*Copyright © 2025 The Author(s): This is an open-access article distributed under the terms of the CC BY-NC 4.0 which permits unrestricted use, distribution, and reproduction in any medium for non-commercial use provided the original author and source are credited*

*Open Access Full Text Article*

Research Article

# Investigation of a Novel PDEδ Inhibitor Targeting K-Ras in Colorectal Cancer: An in Silico and Computer-Aided Drug Design Approach

Mohammed Mouhcine *, Imane Rahnoune, Houda Filali

Laboratory of Pharmacology-Toxicology, Faculty of Medicine and Pharmacy of Casablanca, Hassan II University of Casablanca, Morocco. Laboratory of Scientific and Clinical Research in Cancer Pathologies, CEDoc UH2

## Article Info:

Article History:

Received 18 Aug 2025
Reviewed 11 Oct 2025
Accepted 30 Oct 2025
Published 15 Nov 2025

Cite this article as:

Mouhcine M, Rahnoune I, Filali H, Investigation of a Novel PDEδ Inhibitor Targeting K-Ras in Colorectal Cancer: An in Silico and Computer-Aided Drug Design Approach, Journal of Drug Delivery and Therapeutics. 2025; 15(11):17-30
*DOI:*
*http://dx.doi.org/10.22270/jddt.v15i11.7429*

*For Correspondence:

Mohammed Mouhcine, Laboratory of Pharmacology-Toxicology, Faculty of Medicine and Pharmacy of Casablanca, Hassan II University of Casablanca, Morocco. Laboratory of Scientific and Clinical Research in Cancer Pathologies, CEDoc UH2

## Abstract

**Introduction:** Colorectal cancer is frequently associated with mutations in the KRAS gene, leading to abnormal activation of the KRas protein. Direct targeting of KRas remains a major therapeutic challenge due to the absence of suitable binding sites for small molecules. An alternative strategy involves inhibiting phosphodiesterase δ (PDEδ), a key regulator of KRas oncogenic signaling.

**Objective:** This study aimed to identify novel PDEδ inhibitors through an in silico computer-aided design approach to block the oncogenic signaling of KRas in colorectal cancer.

**Methods:** An integrated computational strategy was used, including pharmacophore modeling based on the crystal structure of PDEδ complexed with an inhibitor, virtual screening of chemical libraries, and drug-likeness filtering according to Lipinski and Veber rules. Selected compounds underwent molecular docking, ADME-Tox prediction, bioavailability assessment, and molecular dynamics simulations (GROMACS) to evaluate stability and binding behavior.

**Results:** The identified hit compound showed strong binding affinity and stable hydrogen interactions with PDEδ. It met all Lipinski and Veber criteria, suggesting good pharmacokinetic potential and oral bioavailability. ADMET analysis revealed a favorable safety profile, and molecular dynamics simulations confirmed its greater stability compared to the co-crystallized ligand.

**Conclusion:**This study identified a promising PDEδ inhibitor capable of interfering with KRas oncogenic signaling in colorectal cancer. These findings provide a solid foundation for the development of new targeted therapies, with future perspectives involving in vitro, in vivo, and clinical validation.

**Keywords:** PDEδ, KRas, Colorectal cancer, Pharmacophore modeling, Virtual screening, Molecular docking, In silico approach, ADMET.

## 1. INTRODUCTION

KRas protein is an oncogenic protein that is encoded by the KRAS gene. This protein has two forms according to its binding state, one active at Guanosine-5'-triphosphate (GTP) and the other inactive at guanosine diphosphate (GDP)[1–3]. When KRas is active, it initiates two vital signaling pathways, RAS/MAPK and PI3K/AKT, that are crucial for controlling cell growth, survival, and proliferation [1,4]. In colorectal cancer, mutations in the KRAS gene occur in roughly 40 to 50% of cases[2,3,5,6]. These mutations prevent the interaction of the KRas protein with the GTPase activator proteins, which are responsible for the hydrolysis of the KRas-bound GTP[3,5,7]. As a result, the KRas protein remains in a constitutively active state, which leads to an abnormal permanent activation of cell proliferation[2,8,9].

The direct targeting of the KRas protein is limited by its small size, its relatively smooth and shallow surface[8,10]. However, research has shown that the KRas protein undergoes post-translational modifications (PTMs) for its localization in the cell membrane and it signaling[11–13]. An important step of these modifications is the farnesylation, which occurs at the level of a cysteine located in the C-terminal CAAX domain (C, cysteine; A, aliphaticaminoacid; X, serine or methionine) of the protein. Farnesylation is carried out by an enzyme called farnesyltransferase[14–16]. After farnesylation, the last three amino acids of the CAAX motif are cleaved by a protease called RCE1 (Ras converting CAAX endopeptidase 1), and the N-terminal farnesylcysteine residue is then methylated by an enzyme called ICMT (isoprenyl cysteine carboxyl methyltransferase)[17–19]. The farnesyl tail attached to the N-terminal cysteine is crucial for KRas to accumulate in the plasma membrane[19–22]. Once farnesylated, the farnesyl tail of KRas is bound by Phosphodiesterase-δ (PDEδ), which facilitates its transport to the plasma membrane. Targeting the PDEδ protein constitutes a promising strategy for blocking the oncogenic signaling of the KRas protein[20–22]. The PDEδ

protein plays a crucial role in the process of localization of KRas in the plasma membrane by binding the farnesyl tail of KRas and facilitating its transport to the membrane[22]. In addition, PDEδ protects this farnesyl tail against proteases present in the cytoplasm, thus maintaining the active form of KRas and thus promoting oncogenic signaling[23–25].

In our research, we employed computational methods including structure-based pharmacophore modeling, virtual pharmacophore-based screening, and molecular docking studies to discover new inhibitors of the PDEδ protein. Our goal was to disrupt oncogenic KRas signaling. The detailed steps of our simulations are shown in Fig. 1.

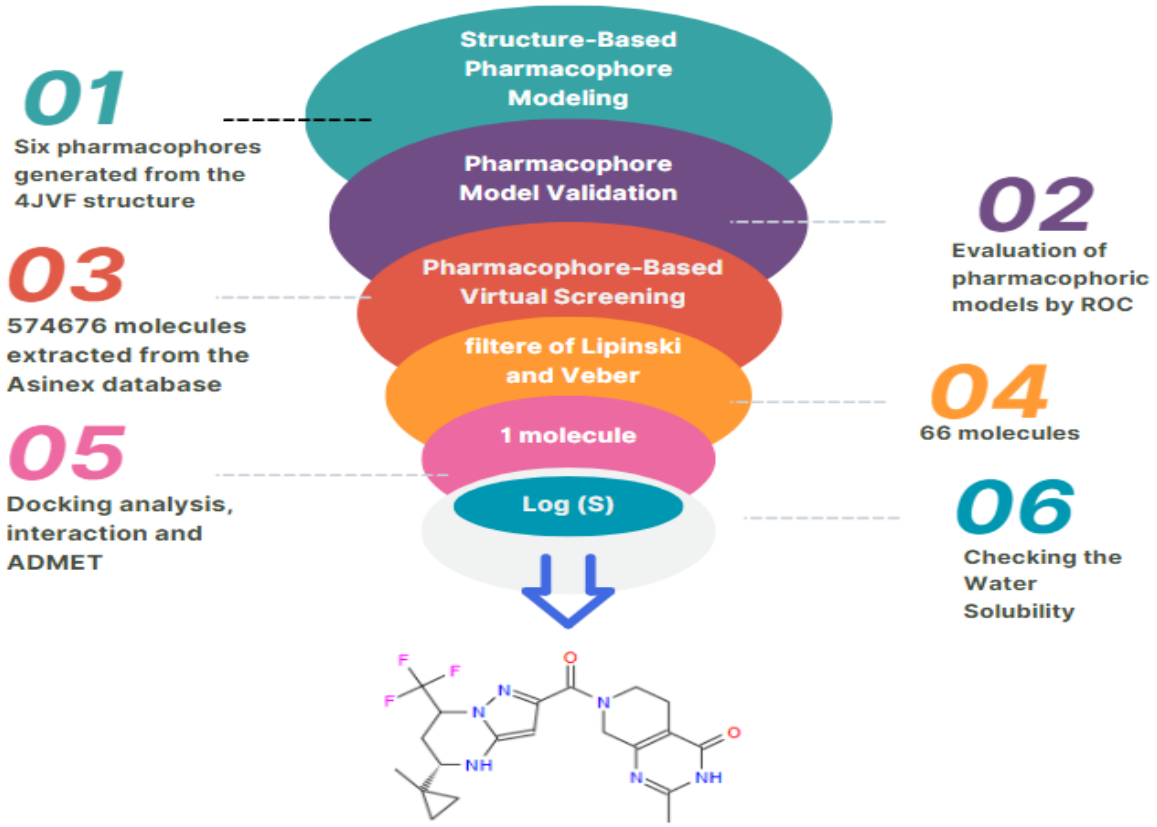


Figure 1: Virtual screening steps implemented in the identification of the inhibition PDEδ.

## 2. MATERIAL AND METHODS

### 2.1. Structure-Based Pharmacophore Modeling

In this study, we undertook the construction of a pharmacophore model based on the crystalline structure of the PDEδ protein in complex with the 17X inhibitor, whose identifier in the PDB database is 4JVF. We used the receptor-ligand pharmacophore generation protocol, integrated into Discovery Studio, for this approach[26]. This protocol is designed to generate pharmacophore models based on the interactions between the receptor and the ligand, thus making it possible to characterize the structural motifs necessary for the biological activity of the inhibitor. The characteristics such as hydrogen bond acceptors, hydrogen bond donors, hydrophobic regions and aromatic rings, corresponding to the interactions between the binding ligand and the protein were used to construct the pharmacophoric models. The parameters of the receptor-ligand pharmacophore generation protocol have been configured as follows: the maximum number of pharmacophores has been set at 10, with a minimum of 4 characteristics and a maximum of 6 characteristics for each pharmacophore generated. Then, the generated pharmacophoric models were classified according to selectivity score. The selectivity of the models was estimated using a genetic function approximation model (GFA), based on a training set of 1544 pharmacophoric models.

### 2.2. Pharmacophore Model Validation

As part of our modeling process, we used the Receiver Operating Characteristic (ROC) curve method to analyze and evaluate the performance of the generated pharmacophoric models. This method, integrated into the software, allows us to measure the ability of our models to differentiate positive results from negative results. The ROC curve, generated by plotting (1-specificity) on the x axis as a function of the sensitivity on the y axis, illustrates the performance of a test in distinguishing between the groups. A random test would produce a diagonal line going from (0,0) to (1,1), which would indicate an absence of discrimination ability. As the accuracy of the test improves, the curve approaches the ideal point of perfect sensitivity and specificity (0.1).

The accuracy is quantified by the area under the curve (AUC), which ranges from 0.5 (random model) to 1.0 (perfect model). Moreover, the area under the curve reflects the probability of correctly identifying the true positives and the true negatives. An ROC score of 0.5 means that the model is random and that it has no predictive utility. We used a dataset comprising 478 molecules, of which 25 were known PDEδ inhibitors obtained from bibliographic research, and the other 428 were molecules with unknown activity randomly selected from the ZINC database (Table 1). Using the area under the ROC curve (AUC), we can evaluate the effectiveness of a pharmacophore in discriminating active molecules from inactive molecules. The AUC scores are often interpreted according to the following criteria: For an AUC between 0.9 and 1.0, the model is qualified as excellent, an AUC between 0.8 and 0.9 is generally considered to be of good quality, When the AUC is between 0.7 and 0.8, the model is considered acceptable, and finally, an AUC between 0.6 and 0.7 indicates a low model quality.

Table 1: The identified PDEδ inhibitors obtained from bibliographic searches.

| Ligands Name | References |
|---|---|
| 18F, 1M1, 1M0, 17X | 27 |
| 5KP | 28 |
| NH6, DL3, 9GD | 29 |
| 8RQ | 30 |
| JAY, P59 | 31 |
| 8SF, 8SL | 32 |
| L8, L7, L4, L3, deltarasin, deltrazinone, Spiperone, atorvastatin, 36l | 33 |
| 1-((2-(3-(7H-Pyrrolo[2,3-d]pyrimidin-4-yl)phenyl)-2-(aminomethyl)-2,3-dihydro-1H-inden-5-yl)methyl) azetidin-3-ol (compound) | pyrimidine derivative |
| 6VO | 34 |
| PD3 | 35 |

### 2.3. Pharmacophore-Based Virtual Screening

The pharmacophore model, whose validity has been confirmed, was used to screen 574676 small molecules extracted from the Asinex database (available on https://www.asinex.com/screening-libraries -(all-libraries)) using the Discovery Studio screen library module. The number of conformations was set at 255, and the conformation method was defined as FAST. The other parameters have been left at the default values. After this step, the candidates who were perfectly aligned with all the characteristics of the pharmacophore were subjected to additional filtering using the Lipinski and Veber rules. These rules provide crucial guidelines for evaluating the potential viability of candidates as drugs, taking into account aspects such as solubility, molecular size and other important properties. All compounds that did not meet these criteria were rejected. No candidate violated the Lipinski or Veber rules, which does not mean that none presented violations.

### 2.4. Analysis of the interactions of hits

To ensure a complete and accurate model of the 4JVF structure, we first reconstructed the six missing residues using ChimeraX 1.9 and Modeller 10.6. This step was essential to restore the integrity of the protein and ensure the reliability of subsequent computational analyses. Molecular docking was then carried out to predict the placement of the hit in the active site of the 4JVF structure, corresponding to the location of the 17X inhibitor. The docking simulations were performed using the GOLD program, chosen for its proven ability to accurately predict ligand-protein binding conformations [36]. The scoring function employed to evaluate the predicted poses was ChemScore, which is widely recognized for its ability to provide reliable estimates of ligand-protein binding affinity. Following the docking, we analyzed the interactions of the hit with PDEδ using the Ligand Interaction Diagram tool in MOE 2015.10.

### 2.5. Prediction of ADME, toxicity, and solubility in water for hits

The candidates selected after the virtual screening based on the pharmacophore will be evaluated using two prediction tools. First of all, the prediction of ADME properties (Absorption, Distribution, Metabolism and Excretion) will be carried out using the SwissADME server, a tool widely used to evaluate the pharmacokinetic properties of chemical compounds[37]. Then, the potential toxicity of the candidates will be evaluated using ProTox 3.0, a server specialized in predicting the toxicity of chemical compounds[38]. These tools will provide essential information on the pharmacokinetics and toxicity of the candidates, thus helping to inform decisions in the drug discovery process. After having carried out the prediction of the ADMET properties, we evaluated the solubility of the hits using the different estimates of the octanol/water partition coefficient (log S) provided by the ESOL, Ali and SILICOS-IT methods. This essential step makes it possible to obtain a complete vision of the pharmacokinetic characteristics of the chemical compounds studied.

### 2.6. Evaluation of the Membrane Permeability of the Hits Resulting from a Virtual Screening Using

After obtaining hits during the virtual screening, we evaluated the Membrane Permeability of the Hits via the PerMM server, a web server and a specialized database, in order to evaluate the passive membrane permeability and the translocation pathways of bioactive molecules as part of this study[39]. This platform offers a complete approach to understanding how molecules interact with cell membranes and cross the lipid barrier.

### 2.7. Evaluation of the stability of the PDEδ-HIT complex

This study evaluates the stability of three systems using molecular dynamics, carried out with the GROMACS software: (1) the PDEδ complex linked to pose 1 of the HIT compound obtained by docking, (2) the PDEδ

complex associated with its 17X co-crystallized ligand, and (3) the PDEδ protein alone, without ligand. The topology of the protein was generated using the CHARMM36 force field, while that of the ligands was obtained thanks to the SwissParam tool. Each system was solvated in a TIP3P water can, with a minimum distance of 1 nm between the protein and the edges of the can. Na+/Cl- ions have been added to neutralize the overall charge of the system.

The balancing of the systems was carried out in two stages under GROMACS: first a balancing in NVT assembly for 100 ps, with a V-scale thermostat to stabilize the temperature at 300 K temperature, then a balancing in NPT assembly for 100 ps to stabilize the pressure at 1 atm. An energy minimization was carried out under GROMACS using the steepest descent algorithm until convergence at a threshold of 1000 in kJ/mol. A production simulation was carried out under GROMACS over a period of 20 ns, with a time step of 2 fs.

The stability of each system was evaluated by calculating the RMSD (Root Mean Square Deviation) and the RMSF (Root Mean Square Fluctuation) of the protein and ligand atoms over time. These analyses were carried out with the GROMACS gmx rms and gmx rmsf tools, and the results were visualized using Grace.

## 3. RESULT

### 3.1. Structure-Based Pharmacophore Modeling and validation

The six pharmacophore models were generated from the crystalline structure of the PDEδ protein in complex with the 17X inhibitor (PDB ID: 4JVF) using the receptor-ligand pharmacophore generation protocol integrated into Discovery Studio (Table 2). Then, we evaluated their selectivity to determine their ability to accurately identify the relevant ligand-protein interactions. The selectivity of each pharmacophore model was estimated using a genetic function approximation model (GFA), based on a training set of 1544 pharmacophore models.

Table 2: Summary of the pharmacophore models for PDEδ.

| Pharmacophore | Number of Features | Feature Set | Selectivity Score |
|---|---|---|---|
| 01 | 5 | AADHH | 9,6184 |
| 02 | 4 | ADHH | 8,1036 |
| 03 | 4 | ADHH | 8,1036 |
| 04 | 4 | AADH | 8,1036 |
| 05 | 4 | AADH | 8,1036 |
| 06 | 4 | AADH | 7,1901 |

After generating the six pharmacophore models from the crystalline structure of the PDEδ protein in complex with the 17X inhibitor (PDB ID: 4JVF), we evaluated their effectiveness in terms of sensitivity and specificity, indicating their ability to correctly identify active and inactive compounds (Figure 3) (Table 3). Among the pharmacophore models generated, the pharmacophore model 2 was selected because of its high AUC (Area Under the Curve) coefficient, estimated at 0.802 (Fig. 2). AUC is a commonly used measure to evaluate the performance of a pharmacophore model, with a value closer to 1 indicating a better predictive ability. The pharmacophore_2 model demonstrated a high sensitivity of 0.88462, indicating its ability to correctly identify the true positives among the active compounds. Moreover, although its specificity is relatively low at 0.056485, the model showed a significant ability to discriminate inactive compounds with only 3 false positives.

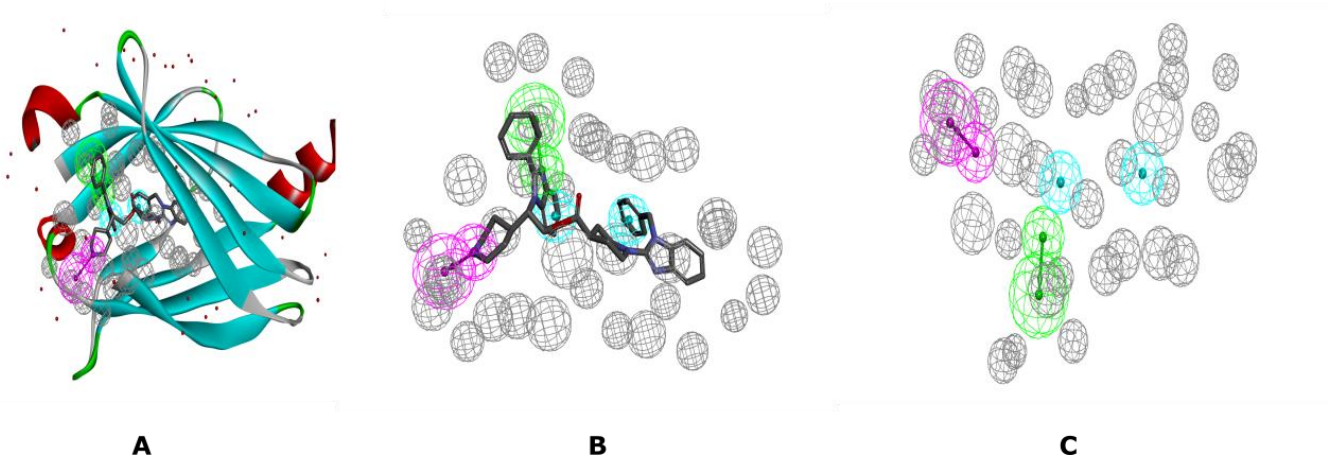


Figure 2: The pharmacophore 2 model generated during the study is characterized by cyan spheres for hydrophobicity, pink for the hydrogen acceptor, green for the hydrogen donor, and gray for the excluded volumes. (A) Crystalline structure of PDEδ (PDB ID: 4JVF) in complex with the 17X co-crystallized ligand and the pharmacophore interaction map. (B) co-crystallized ligand 17X and pharmacophore 2. (C) pharmacophore 2.

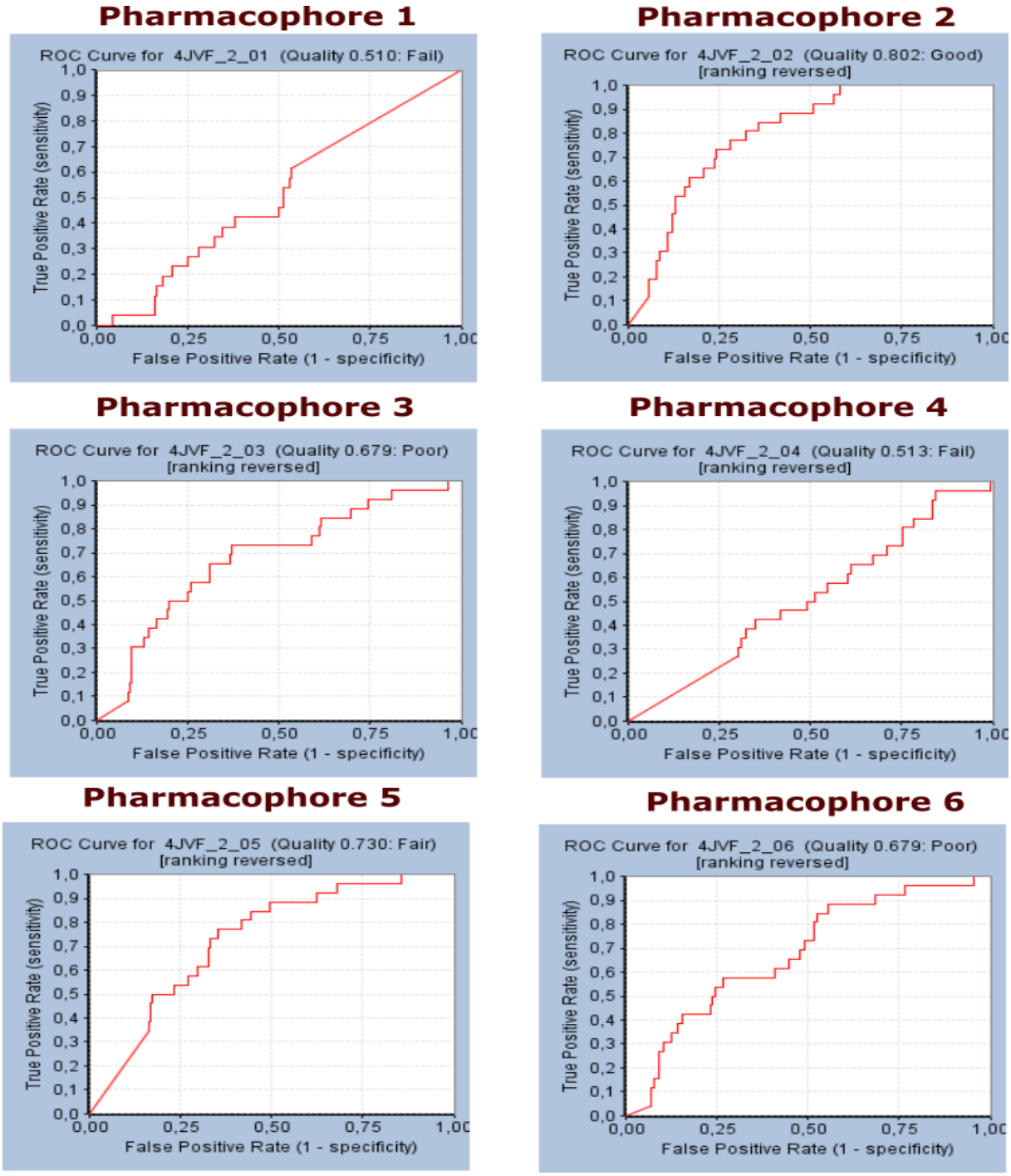


Figure 3: Validation of the six pharmacophore models by the ROC method: Model 2 stands out with an AUC greater than 0.8, qualifying it as the best among the six evaluated models.

Table 3: Validation with Known Assets/Inactives.

| Pharmacophore | Total Actives | Total Inactives | True Positives | True Negatives | False Positives | False Negatives | Sensitivity | Specificity |
|---|---|---|---|---|---|---|---|---|
| Pharmacophore_1 | 26 | 478 | 16 | 222 | 256 | 10 | 0,61538 | 0,46444 |
| Pharmacophore_2 | 26 | 478 | 23 | 27 | 451 | 3 | 0,88462 | 0,056485 |
| Pharmacophore_3 | 26 | 478 | 24 | 39 | 439 | 2 | 0,92308 | 0,081590 |
| Pharmacophore_4 | 26 | 478 | 19 | 143 | 335 | 7 | 0,73077 | 0,29916 |
| Pharmacophore_5 | 26 | 478 | 17 | 78 | 400 | 9 | 0,65385 | 0,16318 |
| Pharmacophore_6 | 26 | 478 | 25 | 31 | 447 | 1 | 0,96154 | 0,064854 |

Following the evaluation of the six pharmacophore models generated, pharmacophore 2 was chosen as the query to screen the Asinex database, containing 574,676 small molecules. This strategic choice is based on the ability of pharmacophore 2 to effectively discriminate between active and inactive compounds, which makes it a valuable tool for the discovery of new therapeutic agents targeting PDEδ protein. The screening of this vast database will make it possible to identify potential candidates who exhibit pharmacophoric interactions similar to those of the 17X inhibitor, thus paving the way for new avenues in the design of drugs targeting this specific target.

### 3.2 Pharmacophore-based Virtual Screening

In our search for new drugs specifically targeting the PDEδ protein, we used the pharmacophore 2 model, which was previously validated during the validation phase (Figure 4A). This model has been applied to the screening of a considerable database, comprising 574,676 small molecules from the Asinex database. Following this initial screening, we identified 66 promising hits presenting a significant correspondence with the specific characteristics of the pharmacophore model. These 66 selected hits will now be evaluated to predict their drug similarity, with the aim of identifying the most promising candidates who share structural similarities or chemical properties with drugs already approved or under development. After screening the candidates according to the strict rules of Lipinski and Veber. Only one hit managed to pass without any violation of these rules (Figure 4B). This hit will now be subjected to a CLINICAL simulation to further evaluate its pharmacological potential and its safety.

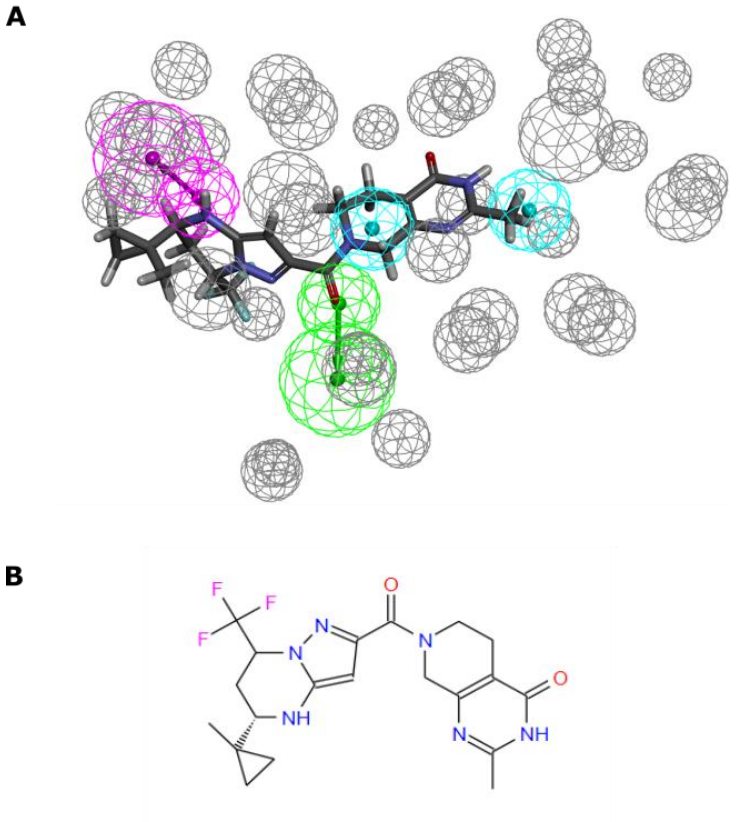


Figure 4: Identification of a new inhibitor of the PDEδ protein. (A) Mapping of hit on the Pharmacophore 2. (B) The hit obtained by the screening.

### 3.1 Docking and interactions analysis of hit

The analysis of the results of the two tables (Table 4 and 5) and of Fig. 5 reveals promising characteristics of hit 1 as a potential inhibitor of the PDEδ protein. First of all, the binding energies calculated for the different poses demonstrate a strong binding affinity between hit 1 and the protein, with negative values indicating a significant stability of the bond. These results are consistent with the idea that hit 1 is able to bind effectively to the active site of the target protein. In addition, the analysis of hydrogen interactions reveals the presence of H-donor and H-acceptor bonds between hit 1 and key residues of the PDEδ protein, such as TYR140, GLU85 and GLN75, in several binding poses. These hydrogen interactions contribute to strengthening the stability of the bond between hit 1 and the protein, which is crucial for its effectiveness as an inhibitor. By combining these observations, we concluded that hit 1 has a strong binding to the active site of the PDEδ protein, reinforced by hydrogen interactions. These results position hit 1 as a promising candidate for an effective inhibitor of the PDEδ protein.

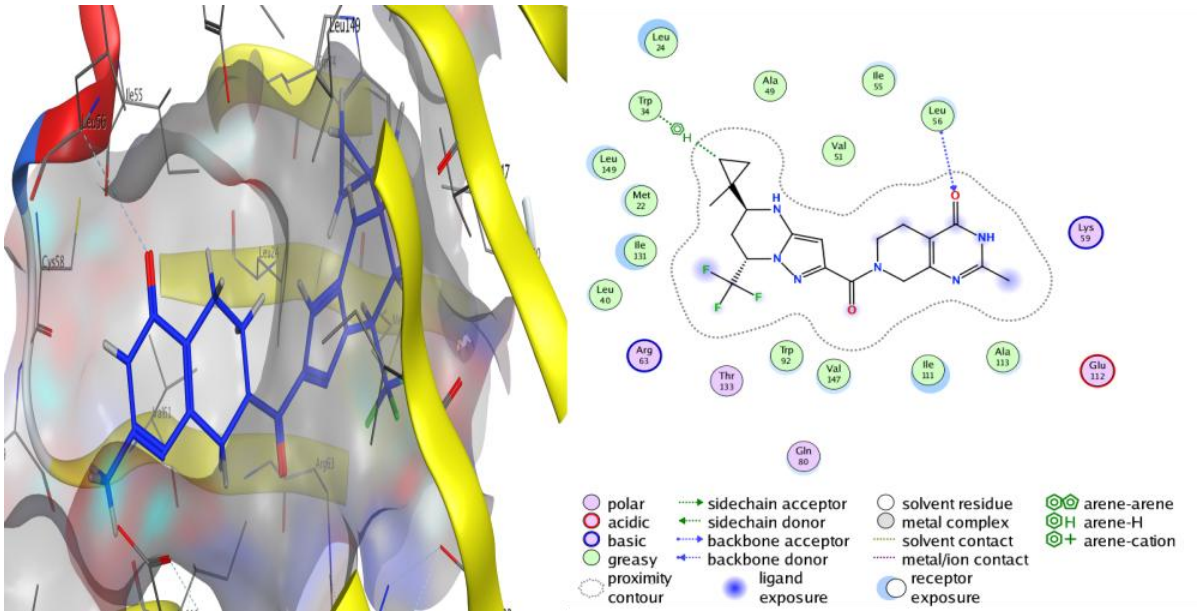


Figure 5: Analysis of the Pose 1 of the Hit by Molecular Docking.

Table 4: Free binding energies of different poses.

| Les Poses | Pose 1 | Pose 2 | Pose 3 | Pose 4 |
|---|---|---|---|---|
| **Free energies of binding calculated by Chemscore (DG bind kJ/mol)** | -27.6282 | -27.3411 | -23.9023 | -23.2998 |

Table 5: Hydrogenic interactions between hit and the PDEδ protein in Various Binding Poses.

| Poses | Ligand Atom | Residue | Protein Atom | Interactions type | Distance | E (kcal/mol) |
|---|---|---|---|---|---|---|
| **1** | O25 | LEU56 | CA | H-acceptor | 3.74 | -0.7 |
| | C21 | TRP34 | 6-ring | H-pi | 4.16 | -0.6 |
| **2** | C20 | TRP92 | 5-ring | H-pi | 4.63 | -0.6 |
| | 5-ring | ILE131 | CG2 | pi-H | 3.81 | -0.7 |
| **3** | O26 | ARG63 | NH1 | H-acceptor | 3.02 | -1.2 |
| | C31 | TRP34 | 6-ring | H-pi | 4.01 | -0.6 |
| **4** | O26 | ARG63 | NH1 | H-acceptor | 3.22 | -1.9 |

### 3.4 ADMET prediction of hit

Based on the pharmacokinetic parameters predicted by the SwissADME server, the selected hit seems to be ideal for optimal pharmacological activity (Table 6). It demonstrates high gastrointestinal absorption. Although its ability to cross the blood-brain barrier (BBB) is not expected, this characteristic could be advantageous to limit adverse effects on the central nervous system. In addition, its negative Log Kp value suggests a limited ability to cross the skin, which could minimize the risks of skin toxicity. Overall, these pharmacokinetic characteristics indicate that the selected hit has a promising potential for drug development, by offering a favorable balance between bioavailability, metabolism and safety.

Table 6: The ADME properties of hit predicted by the SwissADME server.

| GI absorption | BBB permeant | P-gp substrate | CYP1A2 inhibitor | CYP2C19 inhibitor | CYP2C9 inhibitor | CYP2D6 inhibitor | CYP3A4 inhibitor | Log Kp (skin permeation) |
|---|---|---|---|---|---|---|---|---|
| High | No | Yes | No | No | No | Yes | Yes | -7.78 cm/s |

The Bioavailability Radar is a tool used to quickly assess the "drug-likeness" of a molecule. It is based on six physicochemical properties: lipophilicity, size, polarity, solubility, flexibility and saturation. Each of these properties is represented on an axis of the radar, with a physico-chemical range. According to the predictions of the bioavailability radar provided by SwissADME, the hit obtained is located in the optimal zone of the Bioavailability Radar, thus indicating an increased probability of a good bioavailability of the molecule (Figure 6).

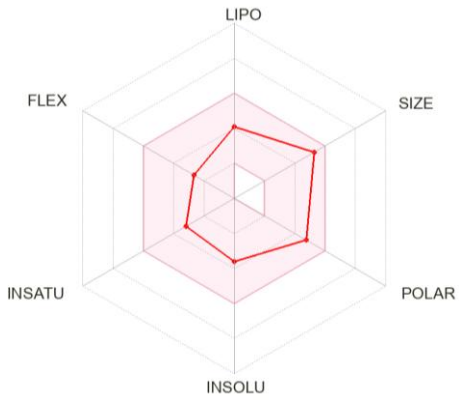


Figure 6: The Radar Bioavailability of hit obtained after the virtual screening. The pink zone represents the optimal range for each physico-chemical property: lipophilicity (XLOGP3 between -0.7 and +5.0), size (MW between 150 and 500 g/mol), polarity (TPSA between 20 and 130 Å2), solubility (log S not exceeding 6), saturation (carbon fraction in sp3 hybridization of at least 0.25), and flexibility (no more than 9 rotary bonds).

### 3.5 Toxicity Analysis

According to the results of ProTox 3.0, presented in Table 7, the hit seems to have a low toxicity for the liver and the heart, with high "Inactive" scores. However, it presents a potential risk of respiratory toxicity, indicated by an "Active" prediction. For other types of toxicity such as carcinogenicity, immunotoxicity, mutagenicity and cytotoxicity, the predictions lean towards inactivity, although some present uncertainty. Overall, these results indicate a generally favorable toxicity profile for hit, but it is important to closely monitor the risk of respiratory toxicity.

Table 7: Prediction of hit toxicity by the ProTox 3.0 web server.

| Classification | Target | Prediction | Probability |
|---|---|---|---|
| Organ toxicity | Hepatotoxicity | Inactive | 0,61 |
| Organ toxicity | Respiratory toxicity | Active | 0,92 |
| Organ toxicity | Cardiotoxicity | Inactive | 0,91 |
| Toxicity end points | Carcinogenicity | Inactive | 0,50 |
| Toxicity end points | Immunotoxicity | Inactive | 0,58 |
| Toxicity end points | Mutagenicity | Inactive | 0,50 |
| Toxicity end points | Cytotoxicity | Inactive | 0,60 |

### 3.6 Water Solubility

Focusing on the different estimates of the octanol/water partition coefficient (log S) provided by the ESOL, Ali, and SILICOS-IT methods, it is clear that hit exhibits consistency in its solubility properties. By examining the solubility classifications, the hit is classified as "Soluble" for the ESOL and Ali methods, and as "Moderately soluble" for the SILICOS-IT method (Table 8). This suggests that hit has a good chance of dissolving effectively in biological media, which is crucial for its absorption and potential as a drug. In summary, the consistent estimates of log S reinforce the favorable perspective of this hit in terms of solubility and bioavailability.

Table 8: Estimates of the octanol/water partition coefficient (log S) for hit according to different methods.

| Methodes | Log (S)( mol/l) | *Class |
|---|---|---|
| **Log S (ESOL)** | -3.59 | Soluble |
| **Log S (Ali)** | -3.29 | Soluble |
| **Log S (SILICOS-IT)** | -4.99 | Moderately soluble |

**Note :** *Solubility Class: Insoluble < -10 < Poorly < -6 < Moderately < -4 < Soluble < -2 Very < 0 < Highly

### 3.7 Evaluation of the Membrane Permeability and the Hit Translocation Path Predicted by the PerMM Server

The results presented in Table 9, resulting from the prediction of hit by the PerMM server, provide important estimates concerning its membrane permeability. They reveal a free binding energy of -3.11 kcal/mol for the DOPC membrane, suggesting a potential affinity of hit with this membrane. In addition, the logarithmic permeability coefficients for different membranes, such as -4.46 for BLM, -4.47 for BBB (Po), -4.62 for CACO2 (Po), -5.34 for PAMPA-DS (Po) and -5.49 for the plasma membrane, offer indications on the ability of hit to cross these biological barriers. These results suggest that hit has a relatively high permeability across different membranes, which could be crucial for its effectiveness as a drug candidate. According to the translocation path of hit illustrated in Fig. 6, it is observed that the hit effectively crosses the plasma membrane and penetrates into the membrane. These observations suggest a promising ability of hit to cross biological barriers, which could be crucial for its pharmacological activity and its therapeutic potential.

Table 9: Parameters calculated by the PerMM server for the evaluation of the membrane permeability of hit.

| Calculated Parameters | |
|---|---|
| Free energy of binding (DOPC) | -3.11 kcal/mol |
| Log of perm. coeff. - BLM | -4.46 |
| Log of perm. coeff - BBB (Po) | -4.47 |
| Log of perm. coeff - CACO2 (Po) | -4.62 |
| Log of perm. coeff - PAMPA-DS (Po) | -5.34 |

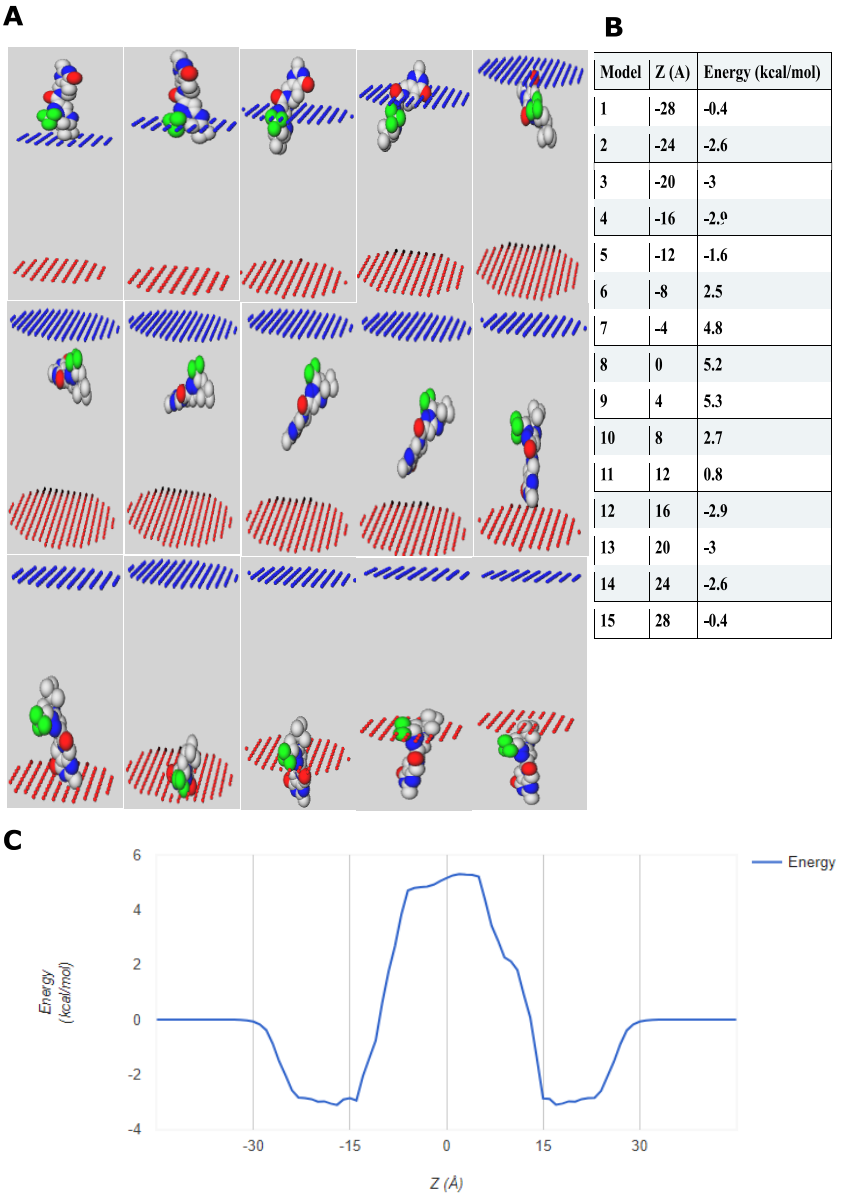


| Model | Z (A) | Energy (kcal/mol) |
|---|---|---|
| 1 | -28 | -0.4 |
| 2 | -24 | -2.6 |
| 3 | -20 | -3 |
| 4 | -16 | -2.9 |
| 5 | -12 | -1.6 |
| 6 | -8 | 2.5 |
| 7 | -4 | 4.8 |
| 8 | 0 | 5.2 |
| 9 | 4 | 5.3 |
| 10 | 8 | 2.7 |
| 11 | 12 | 0.8 |
| 12 | 16 | -2.9 |
| 13 | 20 | -3 |
| 14 | 24 | -2.6 |
| 15 | 28 | -0.4 |

Figure 6: Analysis of the displacement of hit through the lipid bilayer according to the PerMM server. (A)Multiple positions of hit as it moves through the lipid bilayer. (B) Transfer energy of 15 displacement through the lipid bilayer calculated. (C) Graphical representation of the transfer energy profile calculated through the DOPC bilayer, ΔGtranf(z).

### 3.8 Analysis of the Stability of the PDEδ-HIT Complex

The RMSD graph illustrates the structural stability of the three PDEδ systems during a 20 ns molecular dynamics simulation (Figure 7). The analysis shows that the apo PDEδ protein (blue curve) is the most stable, with a low and constant RMSD, indicating a well-conserved structure in the absence of ligand. The PDEδ-HIT complex (green curve) shows initial fluctuations but tends to stabilize after about 5 ns, suggesting a moderately stable interaction between the ligand and the protein. On the other hand, the PDEδ-co-crystallized complex (red curve) displays significant variations in RMSD, with several sudden increases and decreases, reflecting a probable structural instability due to conformational rearrangements or to a weak maintenance of the ligand. These results indicate that the HIT compound could induce a better stability of the PDEδ complex compared to the co-crystallized ligand.

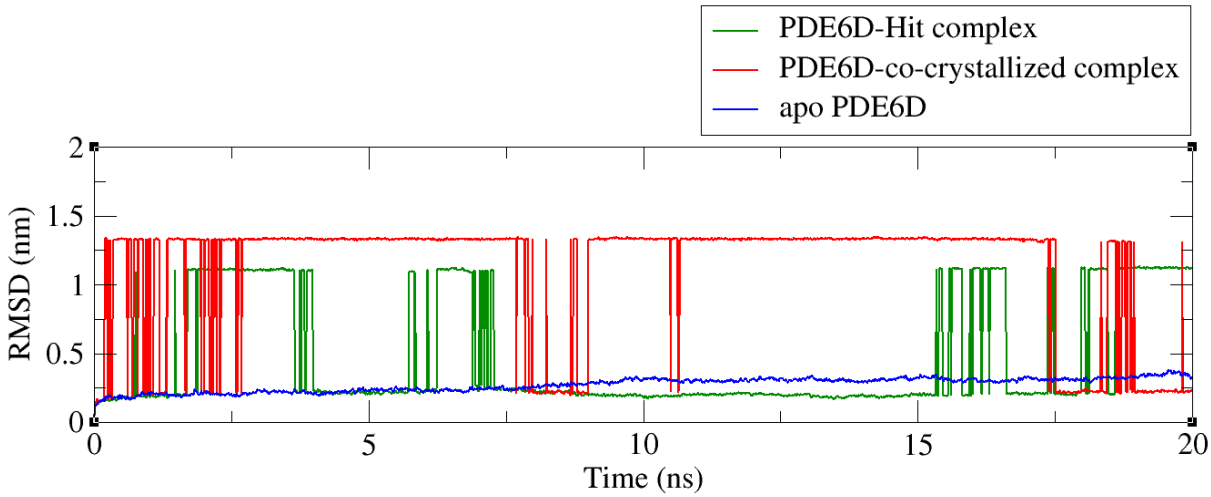


Figure 7: RMSD Analysis of PDEδ Complexes Over a 20 ns Molecular Dynamics Simulation.

Fig. 8 represents the mean fluctuations of the residues (RMSF) of the PDEδ protein during the molecular dynamics simulation. The analysis shows that the majority of the residues show relatively small fluctuations, suggesting a globally stable structure in the three studied systems: apo PDEδ (blue), PDEδ-HIT (green) and PDEδ-co-crystallized (red). However, a significant increase in the RMSF is observed at the C-terminal end (around residue 150), indicating an increased flexibility of this region. This strong fluctuation could be due to the absence of stabilizing interactions with the ligand or to intrinsic movements of the protein in this region. Outside this area, the differences between the three systems remain minimal, suggesting that ligand binding does not strongly affect the flexibility of the majority of the protein structure.

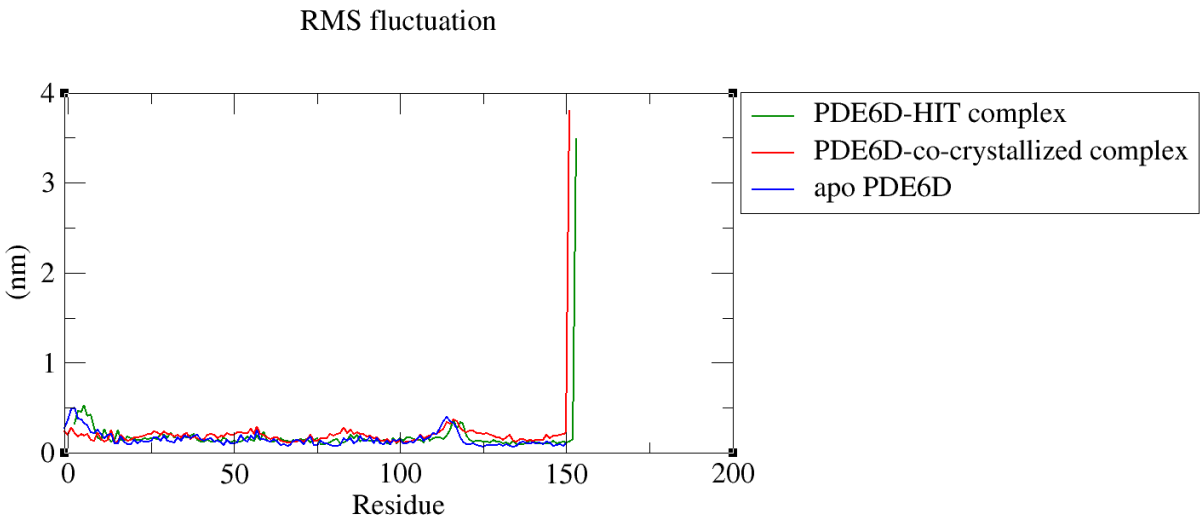


Figure 8: Fluctuation of the residues of the PDEδ protein during the molecular dynamics simulation.

## 4. DISCUSSION

Colorectal cancer frequently involves mutations in the KRAS gene, especially in codons 12 and 13[40]. These mutations, such as the G12C mutation, are associated with a poorer prognosis in metastatic colorectal cancer [41]. KRAS mutations are prevalent in colorectal cancer, with a mutation rate of 37.1%, and are significantly associated with the size of the tumor [42]. Historically considered as "intractable", KRAS mutations in colorectal cancer have experienced breakthroughs with the development of specific covalent inhibitors [43]. Targeting KRAS has always been difficult due to its lack of binding sites to traditional drugs, which makes it difficult and considered "non-druggable"[44,45]. The high affinity of KRas for cellular GTP further complicates the design of the drug, since the single hydrophobic pocket is usually occupied by GDP or GTP, which hinders the binding of small molecules [46]. Recent advances, such as the FDA approval of sotorasib targeting the KRASG12C mutant, have validated KRas as a viable target in oncology [47]. However, common mutations such as G12D and G12V remain difficult to target effectively[48]. Efforts using macrocyclic peptides and CRISPR systems have shown promise in inhibiting KRas signaling and targeting downstream effectors, offering potential therapeutic strategies. Despite these advances, resistance to monotherapy with KRas inhibitors remains an important obstacle, highlighting the need for combination therapies to effectively treat KRAS mutant cancers[49,50].

PTMs play a crucial role in the regulation of KRAS activity [11,51]. These modifications include prenylation, post-prenylation, palmitoylation, ubiquitination, phosphorylation, SUMOylation, acetylation and nitrosylation [52]. The targeting of these post-translational modifications has shown promising antitumor activities, highlighting their importance in the treatment of cancer [53]. In addition, the study of PTMs of KRAS proteins has led to the identification of potential targets for the discovery of anti-RAS drugs, highlighting the importance of understanding these regulatory mechanisms in the development of new therapeutic strategies[54,55] . Also, targeting the membrane localization of KRAS is an effective therapeutic strategy due to the central role of KRAS mutations in various cancers, including colorectal, lung and pancreatic cancers [56–58].

The membrane localization of KRAS is a complex process regulated by several cellular mechanisms[59]. Initially synthesized in the cytoplasm, KRAS is post-traditionally modified by the addition of fatty acids on its C-terminal part, an essential step for its anchoring to the plasma membrane[60,61]. This lipid modification allows KRas to associate closely with the membrane and to exercise its biological functions, in particular its participation in the transduction of the cellular signal[60–62]. In addition, chaperone proteins such as PDEδ facilitate the transport and targeting of KRas to the cell membrane. Once at the membrane, KRas interacts with other membrane proteins to trigger cellular signaling cascades regulating growth, survival and cell differentiation[63–65]. Thus, the membrane localization of KRas is a finely regulated process and crucial for its biological activity[59]. Targeting the interaction between KRas and PDEδ presents a promising strategy to inhibit KRas activities [66]. It has been shown that the inhibition of the interaction between KRas and PDEδ promotes the death of cancer cells [67]. By stabilizing the Ras-PDEδ complex, the redirection of the RAS to the cytoplasm and the primary cil inhibits the oncogenic RAS/ERK signaling, leading to potential anticancer effects [34].

The cellular penetration of PDEδ inhibitors has been the subject of research aimed at improving their effectiveness [68,69]. Strategies such as the engineering of a "chemical spring" in prenyl binding pocket inhibitors and the attachment of cell penetration groups have been used to improve cell penetration [67]. In the context of inhibitors that are effective for passing clinical PDEδ inhibition tests, compounds such as Deltaflexin-1 and -2 have shown promising results[68]. These compounds have been specially designed with a kind of "chemical spring" that makes them more robust and improves their ability to penetrate inside the cells[23,68,70]. Deltaflexin-1 and -2 selectively disrupt the membrane organization of the KRas without affecting the HRas, highlighting their specificity[68,71]. This selectivity profile results in a significant antiproliferative activity on colorectal cancer cells, indicating their potential as effective inhibitors of PDEδ inhibition [68]. Other research has identified small molecules such as DW0254 that inhibit the activation of Ras in leukemia cells by targeting the hydrophobic pocket of PDEδ, resulting in inhibition of Ras and anti-leukemia effects[67].

The discovery of PDEδ inhibitors has been an important focus of cancer research [69]. By specifically blocking PDEδ, it becomes possible to disrupt the molecular mechanisms underlying tumor growth[72–74]. In this regard, the role of protein PDEδ in the localization of KRas to the cell membrane for its normal function. The results obtained during the various stages of our in-silico study for the identification of a new inhibitor of the PDEδ protein, aimed at blocking the oncogenic signaling of the KRas protein in colorectal cancer, have proven to be significant. In addition, this inhibitor has demonstrated an ability to penetrate the plasma membrane (Figure 1). Pharmacophore modeling based on the crystal structure of PDEδ in complex with the inhibitor has made it possible to generate precise models characterizing the key interactions necessary for the biological activity of the inhibitors (Table 4). The virtual screening of vast databases of chemical compounds led to the identification of 66 promising hits, among which one hit was selected after successfully passing the Lipinski and Veber criteria, thus demonstrating its compliance with pharmacological and safety standards (Figure 4). The analysis of the interactions by molecular docking revealed a strong binding affinity between the selected hit and PDEδ, confirming its ability to bind effectively to the active site of the target protein (Figure 5) (Table 4 and 5). In addition, the evaluation of the membrane permeability of hit has provided essential information on its ability to cross cell membranes, reinforcing its potential as an inhibitor of oncogenic KRas signaling (Figure 6). The analysis of the results of RMSD and RMSF shows a better stability of the PDEδ-HIT complex

compared to the co-crystallized complex(figure 7 and 8). Indeed, the RMSD of PDEδ-HIT remains relatively stable after 5 ns, while that of the co-crystallized complex exhibits significant fluctuations, suggesting a less stable interaction with the protein. Moreover, the fluctuations of the residues (RMSF) are similar between the systems, except at the level of the C-terminal end, where a strong variability is observed. This local instability may be due to the absence of structural constraints or to an intrinsic flexibility of this region. The PDEδ apo shows superior stability, which is expected in the absence of a ligand that can induce conformational rearrangements. The better stability of the HIT complex suggests that this ligand interacts more favorably with PDEδ, maintaining its structure more efficiently than the co-crystallized ligand, which was however the experimental reference.

These results underline the effectiveness of in silico approaches for the discovery of new therapeutic agents targeting critical oncogenic pathways, thus paving the way for future translational studies for the treatment of colorectal cancer. Despite the progress made in the development of PDEδ inhibitors with improved affinities and selectivity, challenges remain to achieve optimal cell penetration for effective therapeutic results[75]. Further research is needed to improve the effectiveness of PDEδ inhibitors for potential clinical applications[75].

## 5. CONCLUSION

The study presents an innovative approach to target the oncogenic signaling of the KRas protein in colorectal cancer by identifying new inhibitors of the PDEδ protein.The results demonstrate a strong pharmacological potential of the identified inhibitor, indicating promising prospects for the development of new therapeutic strategies to treat colorectal cancer by disrupting the molecular mechanisms involved in tumor growth. Future prospects could include in vitro and in vivo studies to validate the efficacy and safety of this inhibitor, as well as clinical trials to evaluate its therapeutic potential in colorectal cancer patients with KRas mutations.

### List of Abbreviations

**ADME:** Absorption, Distribution, Metabolism, Excretion ADMET: Absorption, Distribution, Metabolism, Excretion, and Toxicity

**AUC:** Area Under the Curve ESOL: Estimated log S

**GOLD:** Genetic Optimization for Ligand Docking

**GTP:** Guanosine Triphosphate

**KRas:** Kirsten Rat Sarcoma Viral Oncogene Homolog

**PDEδ:** Phosphodiesterase delta

**PI3K/AKT:** Phosphatidylinositol 3-Kinase/Protein Kinase B

**ROC:** Receiver Operating Characteristic

**Ethics Approval and Consent to Participate:** Not applicable.

**Human and Animal Rights:** No animals/humans were used in the studies that are the basis of this research.

**Consent For Publication:** Not applicable.

**Availability of Data and Materials:** The data and supportive information are available within the article.

**Funding:** None.

**Conflict Of Interest:** The authors declare no conflict of interest, financial or otherwise.

**Acknowledgements:** Declared none.

**Author's Contribution:** study conception and design : Mohammed MOUHCINE, Imane RAHMOUNE, Houda FILALI. All authors reviewed the results and approved the final version of the manuscript.

## REFERENCES

1. Kim HJ, Lee HN, Jeong MS, Jang SB, Oncogenic KRAS: signaling and drug resistance, Cancers, 2021; 13:5599 https://doi.org/10.3390/cancers13225599 PMid:34830757 PMCid:PMC8616169

2. McCormick F, Targeting KRAS directly, Annu Rev Cancer Biol, 2018; 2:81-90 https://doi.org/10.1146/annurev-cancerbio-050216-122010

3. Menyhárd DK, et al., Structural impact of GTP binding on downstream KRAS signaling, Chem Sci, 2020; 11:9272-9289 https://doi.org/10.1039/D0SC03441J PMid:34094198 PMCid:PMC8161693

4. Cuesta C, Arévalo-Alameda C, Castellano E, The importance of being PI3K in the RAS signaling network, Genes, 2021; 12:1094 https://doi.org/10.3390/genes12071094 PMid:34356110 PMCid:PMC8303222

5. Benhattar J, Losi L, Chaubert P, Givel JC, Costa J, Prognostic significance of K-ras mutations in colorectal carcinoma, Gastroenterology, 1993; 104:1044-1048 https://doi.org/10.1016/0016-5085(93)90272-E PMid:8462792

6. Liu X, Jakubowski M, Hunt JL, KRAS gene mutation in colorectal cancer is correlated with increased proliferation and spontaneous apoptosis, Am J Clin Pathol, 2011; 135:245-252 https://doi.org/10.1309/AJCP7FO2VAXIVSTP PMid:21228365

7. Hunter JC, et al., Biochemical and structural analysis of common cancer-associated KRAS mutations, Mol Cancer Res, 2015; 13:1325-1335 https://doi.org/10.1158/1541-7786.MCR-15-0203 PMid:26037647

8. Chen H, Smaill JB, Liu T, Ding K, Lu X, Small-molecule inhibitors directly targeting KRAS as anticancer therapeutics, J Med Chem, 2020; 63:14404-14424 https://doi.org/10.1021/acs.jmedchem.0c01312 PMid:33225706

9. Bryant KL, Mancias JD, Kimmelman AC, Der CJ, KRAS: feeding pancreatic cancer proliferation, Trends Biochem Sci, 2014; 39:91-100 https://doi.org/10.1016/j.tibs.2013.12.004 PMid:24388967 PMCid:PMC3955735

10. Huang L, Guo Z, Wang F, Fu L, KRAS mutation: from undruggable to druggable in cancer, Signal Transduct Target Ther, 2021; 6:1-20 https://doi.org/10.1038/s41392-021-00780-4 PMid:34776511 PMCid:PMC8591115

11. Wang W, et al., Post-translational modification of KRAS: potential targets for cancer therapy, Acta Pharmacol Sin, 2021; 42:1201-1211 https://doi.org/10.1038/s41401-020-00542-y PMid:33087838 PMCid:PMC8285426

12. Campbell SL, Philips MR, Post-translational modification of RAS proteins, Curr Opin Struct Biol, 2021; 71:180-192 https://doi.org/10.1016/j.sbi.2021.06.015 PMid:34365229 PMCid:PMC8649064

13. Ahearn IM, Haigis K, Bar-Sagi D, Philips MR, Regulating the regulator: post-translational modification of RAS, Nat Rev Mol Cell Biol, 2012; 13:39-51 https://doi.org/10.1038/nrm3255 PMid:22189424 PMCid:PMC3879958

14. Friday BB, Adjei AA, K-ras as a target for cancer therapy, Biochim Biophys Acta, 2005; 1756:127-144 https://doi.org/10.1016/j.bbcan.2005.08.001 PMid:16139957

15. Asati V, Mahapatra DK, Bharti SK, K-Ras and its inhibitors towards personalized cancer treatment: Pharmacological and structural perspectives, Eur J Med Chem, 2017; 125:299-314 https://doi.org/10.1016/j.ejmech.2016.09.049 PMid:27688185

16. Sinensky M, Lutz RJ, The prenylation of proteins, Bioessays, 1992; 14:25-31 https://doi.org/10.1002/bies.950140106 PMid:1546978

17. Xiang S, Bai W, Bepler G, Zou X, Activation of Ras by Post-Translational Modifications, Conquering RAS, 2017; 97-118 https://doi.org/10.1016/B978-0-12-803505-4.00006-0 PMid:28733654 PMCid:PMC5522455

18. Korzeniecki C, Priefer R, Targeting KRAS mutant cancers by preventing signaling transduction in the MAPK pathway, Eur J Med Chem, 2021; 211:113006 https://doi.org/10.1016/j.ejmech.2020.113006 PMid:33228976

19. Eng SK, Loh THT, Goh BH, Lee WL, KRAS as potential target in colorectal cancer therapy, Natural Bio-active Compounds, 2019; 1:389-424 https://doi.org/10.1007/978-981-13-7154-7_12

20. Jang H, et al., Mechanisms of membrane binding of small GTPase K-Ras4B farnesylated hypervariable region, J Biol Chem, 2015; 290:9465-9477 https://doi.org/10.1074/jbc.M114.620724 PMid:25713064 PMCid:PMC4392252

21. Parker JA, Mattos C, The Ras-membrane interface: isoform-specific differences in the catalytic domain, Mol Cancer Res, 2015; 13:595-603 https://doi.org/10.1158/1541-7786.MCR-14-0535 PMid:25566993

22. Schmick M, Kraemer A, Bastiaens PIH, Ras moves to stay in place, Trends Cell Biol, 2015; 25:190-197 https://doi.org/10.1016/j.tcb.2015.02.004 PMid:25759176

23. Siddiqui FA, Development of Novel Drugs Targeting Chaperones of Oncogenic K-Ras, 2021

24. Schmick M, et al., KRas localizes to the plasma membrane by spatial cycles of solubilization, trapping and vesicular transport, Cell, 2014; 157:459-471 https://doi.org/10.1016/j.cell.2014.02.051 PMid:24725411

25. Dharmaiah S, et al., Structural basis of recognition of farnesylated and methylated KRAS4b by PDEδ, Proc Natl Acad Sci, 2016; 113:E6766-E6775 https://doi.org/10.1073/pnas.1615316113 PMid:27791178 PMCid:PMC5098621

26. Jejurikar BL, Rohane SH, Drug designing in discovery studio, 2021

27. Zimmermann G, et al., Small molecule inhibition of the KRAS-PDEδ interaction impairs oncogenic KRAS signalling, Nature, 2013; 497:638-642 https://doi.org/10.1038/nature12205 PMid:23698361

28. Papke B, et al., Identification of pyrazolopyridazinones as PDEδ inhibitors, Nat Commun, 2016; 7:11360 https://doi.org/10.1038/ncomms11360 PMid:27094677 PMCid:PMC4843002

29. Martín-Gago P, et al., A PDE6δ-KRas inhibitor chemotype with up to seven H-bonds and picomolar affinity that prevents efficient inhibitor release by Arl2, Angew Chem, 2017; 129:2463-2468 https://doi.org/10.1002/ange.201610957

30. Martín-Gago P, et al., Covalent protein labeling at glutamic acids, Cell Chem Biol, 2017; 24:589-597 https://doi.org/10.1016/j.chembiol.2017.03.015 PMid:28434875

31. Jiang Y, et al., Structural biology-inspired discovery of novel KRAS-PDEδ inhibitors, J Med Chem, 2017; 60:9400-9406 https://doi.org/10.1021/acs.jmedchem.7b01243 PMid:28929751

32. Bing X, et al., Fragment-based Drug Discovery of inhibitors to block PDEdelta-RAS protein-protein interaction

33. Chen L, et al., Discovery of novel KRAS-PDEδ inhibitors with potent activity in patient-derived human pancreatic tumor xenograft models, Acta Pharm Sin B, 2022; 12:274-290 https://doi.org/10.1016/j.apsb.2021.07.009 PMid:35127385 PMCid:PMC8799878

34. Yelland T, et al., Stabilization of the ras: Pde6d complex is a novel strategy to inhibit ras signaling, J Med Chem, 2022; 65:1898-1914 https://doi.org/10.1021/acs.jmedchem.1c01265 PMid:35104933 PMCid:PMC8842248

35. Lee J, et al., Development of PD3 and PD3-B for PDEδ inhibition to modulate KRAS activity, J Enzyme Inhib Med Chem, 2022; 37:1656-1666 https://doi.org/10.1080/14756366.2022.2086865 PMid:35695156 PMCid:PMC9225715

36. Verdonk ML, Cole JC, Hartshorn MJ, Murray CW, Taylor RD, Improved protein-ligand docking using GOLD, Proteins, 2003; 52:609-623 https://doi.org/10.1002/prot.10465 PMid:12910460

37. Daina A, Michielin O, Zoete V, SwissADME: a free web tool to evaluate pharmacokinetics, drug-likeness and medicinal chemistry friendliness of small molecules, Sci Rep, 2017; 7:42717 https://doi.org/10.1038/srep42717 PMid:28256516 PMCid:PMC5335600

38. Banerjee P, Eckert AO, Schrey AK, Preissner R, ProTox-II: a webserver for the prediction of toxicity of chemicals, Nucleic Acids Res, 2018; 46:W257-W263 https://doi.org/10.1093/nar/gky318 PMid:29718510 PMCid:PMC6031011

39. Lomize AL, et al., PerMM: A web tool and database for analysis of passive membrane permeability and translocation pathways of bioactive molecules, J Chem Inf Model, 2019; 59:3094-3099 https://doi.org/10.1021/acs.jcim.9b00225 PMid:31259547 PMCid:PMC6781619

40. Ottaiano A, et al., KRAS p. G12C Mutation in Metastatic Colorectal Cancer: Prognostic Implications and Advancements in Targeted Therapies, Cancers, 2023; 15:3579 https://doi.org/10.3390/cancers15143579 PMid:37509241 PMCid:PMC10377118

41. Cao Y, et al., Construction of prediction model for KRAS mutation status of colorectal cancer based on CT radiomics, Jpn J Radiol, 2023; 41:1236-1246 https://doi.org/10.1007/s11604-023-01458-3 PMid:37311935 PMCid:PMC10613595

42. Wu C, et al., Advances in KRAS mutation inhibition in metastatic colorectal cancer, Holistic Integr Integr Oncol, 2023; 2:14 https://doi.org/10.1007/s44178-023-00032-1

43. Ren Z, Che J, Wu XW, Xia J, Analysis of KRAS mutation status prediction model for colorectal cancer based on medical imaging, Comput Math Methods Med, 2021 https://doi.org/10.1155/2021/3953442 PMid:34976107 PMCid:PMC8716224

44. Negri F, Bottarelli L, de'Angelis GL, Gnetti L, KRAS: a druggable target in colon cancer patients, Int J Mol Sci, 2022; 23:4120 https://doi.org/10.3390/ijms23084120 PMid:35456940 PMCid:PMC9027058

45. Lim S, et al., Discovery of cell active macrocyclic peptides with on-target inhibition of KRAS signaling, Chem Sci, 2021; 12:15975-15987 https://doi.org/10.1039/D1SC05187C PMid:35024121 PMCid:PMC8672774

46. Bender G, Fahrioglu Yamaci R, Taneri B, CRISPR and KRAS: a match yet to be made, J Biomed Sci, 2021; 28:1-25 https://doi.org/10.1186/s12929-021-00772-0 PMid:34781949 PMCid:PMC8591907

47. Zhu C, et al., Targeting KRAS mutant cancers: from druggable therapy to drug resistance, Mol Cancer, 2022; 21:159 https://doi.org/10.1186/s12943-022-01629-2 PMid:35922812 PMCid:PMC9351107

48. Bear AS, et al., Mutant KRAS-specific T cell receptors directed against prevalent G12D and G12V variants exhibit potent cytotoxic activity and CD8 co-receptor independence, Cancer Res, 2022; 82:PR019-PR019 https://doi.org/10.1158/1538-7445.PANCA22-PR019

49. Yau EH, et al., Genome-wide CRISPR screen for essential cell growth mediators in mutant KRAS colorectal cancers, Cancer Res,

2017; 77:6330-6339 https://doi.org/10.1158/0008-5472.CAN-17-2043 PMid:28954733 PMCid:PMC5690866

50. Punekar SR, Velcheti V, Neel BG, Wong KK, The current state of the art and future trends in RAS-targeted cancer therapies, Nat Rev Clin Oncol, 2022; 19:637-655 https://doi.org/10.1038/s41571-022-00671-9 PMid:36028717 PMCid:PMC9412785

51. Bortoletto A, et al., Oncogenic KRAS promotes pancreatic ductal adenocarcinoma through post-transcriptionally regulated KRAS-induced granules (KGs), 2023 https://doi.org/10.21203/rs.3.rs-3064215/v1

52. Ahearn I, Zhou M, Philips MR, Posttranslational modifications of RAS proteins, Cold Spring Harb Perspect Med, 2018; 8 https://doi.org/10.1101/cshperspect.a031484 PMid:29311131 PMCid:PMC6035883

53. Ma Y, Xu J, Huang P, Bai X, Gao H, Ubiquitin-independent, Proteasome-mediated targeted degradation of KRAS in pancreatic adenocarcinoma cells using an engineered ornithine decarboxylase/antizyme system, IUBMB Life, 2019; 71:57-65 https://doi.org/10.1002/iub.1945 PMid:30347501 PMCid:PMC7379993

54. Yang Y, Jiao Y, Mohammadi MR, Post-translational modifications of proteins in tumor immunotherapy and their potential as immunotherapeutic targets, Cell Mol Biomed Rep, 2023; 3:172-184 https://doi.org/10.55705/cmbr.2023.378480.1091

55. Wadood A, Ajmal A, Rehman AU, Strategies for Targeting KRAS: A Challenging Drug Target, Curr Pharm Des, 2022; 28:1897-1901 https://doi.org/10.2174/1381612828666220506144046 PMid:35524675

56. Lam KK, et al., KRAS-specific antibody binds to KRAS protein inside colorectal adenocarcinoma cells and inhibits its localization to the plasma membrane, Front Oncol, 2023; 13:1000 https://doi.org/10.3389/fonc.2023.1036871 PMid:37051535 PMCid:PMC10084885

57. Kaya P, et al., Drug targeting of KRAS accumulation on the cilium inhibits its stemness driving activity, Cancer Res, 2023; 83:3493 https://doi.org/10.1158/1538-7445.AM2023-3493

58. Singh N, et al., Targeting RAS beyond KRAS, a review, Mol Cancer Res, 2023; 21:A032-A032 https://doi.org/10.1158/1557-3125.RAS23-A032

59. Liu J, et al., Glycolysis regulates KRAS plasma membrane localization and function through defined glycosphingolipids, Nat Commun, 2023; 14:465 https://doi.org/10.1038/s41467-023-36128-5 PMid:36709325 PMCid:PMC9884228

60. Messing S, et al., Production and membrane binding of N-terminally acetylated, C-terminally farnesylated and carboxymethylated KRAS4b, Ras Activity and Signaling: Methods and Protocols, 2021; 105-116 https://doi.org/10.1007/978-1-0716-1190-6_6 PMid:33977473

61. Zhou Y, Prakash PS, Liang H, Gorfe AA, Hancock JF, The KRAS and other prenylated polybasic domain membrane anchors recognize phosphatidylserine acyl chain structure, Proc Natl Acad Sci, 2021; 118:e2014605118 https://doi.org/10.1073/pnas.2014605118 PMid:33526670 PMCid:PMC8017956

62. Lee K, Ikura M, Marshall CB, The Self-Association of the KRAS4b Protein is Altered by Lipid-Bilayer Composition and Electrostatics, Angew Chem, 2023; 135:e202218698 https://doi.org/10.1002/ange.202218698

63. Henkels KM, Rehl KM, Cho K, Blocking K-ras interaction with the plasma membrane is a tractable therapeutic approach to inhibit oncogenic K-ras activity, Front Mol Biosci, 2021; 8:673096 https://doi.org/10.3389/fmolb.2021.673096 PMid:34222333 PMCid:PMC8244928

64. Cabot D, Analysis of KRAS phosphorylation and KRAS effector domain as targets for cancer therapy, 2020

65. Liu P, Wang Y, Li X, Targeting the untargetable KRAS in cancer therapy, Acta Pharm Sin B, 2019; 9:871-879 https://doi.org/10.1016/j.apsb.2019.03.002 PMid:31649840 PMCid:PMC6804475

66. Holderfield M, Efforts to develop KRAS inhibitors, Cold Spring Harb Perspect Med, 2018; 8:a031864 https://doi.org/10.1101/cshperspect.a031864 PMid:29101115 PMCid:PMC6027934

67. Canovas Nunes S, et al., Validation of a small molecule inhibitor of PDE6D-RAS interaction with favorable anti-leukemic effects, Blood Cancer J, 2022; 12:64 https://doi.org/10.1038/s41408-022-00663-z PMid:35422065 PMCid:PMC9010429

68. Siddiqui FA, et al., PDE6D inhibitors with a new design principle selectively block K-Ras activity, ACS Omega, 2019; 5:832-842 https://doi.org/10.1021/acsomega.9b03639 PMid:31956834 PMCid:PMC6964506

69. Li Y, et al., Identification of PDE6D as a potential target of sorafenib via PROTAC technology, bioRxiv, 2020-2025 https://doi.org/10.1101/2020.05.06.079947

70. Majrashi TA, et al., DFT and molecular simulation validation of the binding activity of PDEδ inhibitors for repression of oncogenic K-Ras, PLoS One, 2024; 19:e0300035 https://doi.org/10.1371/journal.pone.0300035 PMid:38457483 PMCid:PMC10923412

71. Lin WC, et al., H-Ras forms dimers on membrane surfaces via a protein-protein interface, Proc Natl Acad Sci, 2014; 111:2996-3001 https://doi.org/10.1073/pnas.1321155111 PMid:24516166 PMCid:PMC3939930

72. Bello M, Correa-Basurto J, Vargas-Mejía MA, Molecular mechanism of the association and dissociation of Deltarasin from the heterodimeric KRas4B-PDEδ complex, Biopolymers, 2019; 110:e23333 https://doi.org/10.1002/bip.23333 PMid:31568570

73. Leung EL, et al., Identification of a new inhibitor of KRAS-PDEδ interaction targeting KRAS mutant nonsmall cell lung cancer, Int J Cancer, 2019; 145:1334-1345 https://doi.org/10.1002/ijc.32222 PMid:30786019

74. Klein CH, et al., PDEδ inhibition impedes the proliferation and survival of human colorectal cancer cell lines harboring oncogenic KRas, Int J Cancer, 2019; 144:767-776 https://doi.org/10.1002/ijc.31859 PMid:30194764 PMCid:PMC6519276

75. Bondarev AD, et al., Recent developments of phosphodiesterase inhibitors: Clinical trials, emerging indications and novel molecules, Front Pharmacol, 2022; 13:1057083 https://doi.org/10.3389/fphar.2022.1057083 PMid:36506513 PMCid:PMC9731127